Airload, Blade Response, and Hub Force Measurements on the NH-3A Compound Helicopter

RONALD R. FENAUGHTY* AND EDWARD A. BENO†
Sikorsky Aircraft Division, United Aircraft Corporation, Stratford, Conn.

This paper summarizes the results of the NH-3A high-speed compound helicopter rotor loads flight-test program supported by NASC and USAAVLABS. The aircraft was instrumented to measure: blade aerodynamic pressures on the main rotor blade; blade response in the flatwise, edgewise, and torsion directions; hub forces using a blade root response measurement method; and airframe response. Rotor advance ratio, lift, and propulsion were varied to determine their effects on rotor loads and vibration. Data were acquired at airspeeds as high as 185 knots to provide data required for high-speed compound design. Results are shown of a correlation study comparing test data with analytic data obtained from a Sikorsky blade dynamic analysis, coupled with a variable inflow program originally developed by Cornell Aeronautical Laboratory and modified by United Aircraft Corporation Research Laboratories (UACRL). Hub forces were successfully measured using the blade root response method. Vibratory in-plane rotor hub forces are much higher than the vertical forces and increase with increase in airspeed, whereas the vertical forces are insensitive to airspeed. Increasing rotor lift or advance ratio increases vibratory hub forces and blade bending moments, whereas a lesser effect is seen due to variation in rotor propulsion.

Nomenclature

b	=	number of blades
C_D/σ	=	main rotor drag coefficient/solidity ratio
C_T/σ	=	main rotor thrust coefficient/solidity ratio
F	=	force
k	=	any integer; 0, 1, 2, 3, . . .
M_y	=	blade flatwise bending moment
M_z	=	blade edgewise bending moment
n/rev	=	number of blades × the main rotor angular velocity
T_0	=	steady blade tension
x_{B-1}	=	blade radial distance from inboard end of instrumented segment to center of gravity of instrumented segment
Δx	=	length of instrumented segment
z	=	vertical deflection in blade axis system
β	=	blade root flap angle
γ	=	blade root lead-lag angle
μ	=	advance ratio
ψ	=	azimuth angle
Ω	=	rotor angular velocity
$(\ )_B$	=	at center of gravity of instrumented segment
$(\ )_c$	=	at center of gravity of cuff
$(\ )_H$	=	pertaining to the main rotor hub
$(\ )_n$	=	nth harmonic
$(\ )_{x,y,z}$	=	parameter in blade axis system; x radial, y tangential, z vertical
$(\ )_{X,Y,Z}$	=	parameter in hub nonrotating axis system; X longitudinal, Y lateral, Z vertical
$(\ )_0$	=	at the blade hinge point (root)
$(\ )_1$	=	at the inboard end of the instrumented segment
$(\ )_3$	=	at the outboard end of the instrumented segment
$(\ )^R$	=	parameter in the hub rotating system with origin at the shaft
$(\ )^*$	=	parameter in the hub rotating system with origin at the lag-flap hinge

Presented as Paper 68-980 at the AIAA 5th Annual Meeting and Technical Display, Philadelphia, Pa., October 21, 1968; submitted November 12, 1968; revision received May 15, 1969. This work was supported by NASC and USAAVLABS under Contract NOw 64-0528-f, C/N 5368-65.

* Supervisor, Rotor Structural Dynamics Group.
† Structural Mechanics Engineer, Structural Mechanics and Methods Group.

Introduction

SIKORSKY Aircraft recently conducted a flight research program to investigate the dynamics of a compound helicopter system going from the aerodynamic excitation of the main rotor blade to the resulting vibratory airframe response. High-speed flights of the NH-3A, a research compound helicopter, provided an evaluation of the effects of rotor lift and drag as well as of advance ratio for speeds in excess of 200 mph.

Related studies have recently been completed. Airloads, blade response, and hub loads have been measured on a tandem rotor helicopter.[1] Rigid rotor compound helicopter blade airloads and response have also been measured.[2] The program described herein measured this dynamic data for a compound helicopter with articulated single main rotor.

Only a brief description of the NH-3A rotor loads program can be presented here. Detailed description of methods and compilation of all of the data are included in the program report.[3]

Data Acquisition/Reduction

The data that were collected during this program are shown schematically in Fig. 1. Blade aerodynamic loading was measured by miniature semiconductor pressure gages. These are highly sensitive, temperature compensating transducers, recently developed by Scientific Advances Inc., that provide accurate dynamic pressure measurement. The structural integrity of the blade is not affected because these minute gages are bonded to the external surface of the blade. Blade response was measured by standard strain gages along the span of the blade and angulators at the blade root. Rotor hub forces were calculated from measurements of blade root bending and angular acceleration, blade tension, and hub acceleration. Airframe response was measured by standard linear accelerometers.

Over 90 dynamic parameters were recorded on magnetic tape. Information required to define the environment of the aircraft was recorded on a photopanel. Complete chordwise pressure distributions were obtained at five spanwise locations. Emphasis was placed on measurement of airloads at the tip of the blade since earlier studies had indicated that correct

definition of tip airloading is essential in order to adequately define n/rev blade response and the resulting hub forces.

The flight-test envelope included variation of rotor lift and drag at advance ratios of 0.36, 0.42, and 0.47. The compound flight program was performed by holding advance ratio and collective pitch constant and varying the elevator or wing flap positions in order to vary rotor lift and drag. Cyclic pitch was adjusted to maintain level flight. Auxiliary propulsion was changed in order to provide the required total propulsive force. Several variations of elevator and wing flaps were made at each of three values of collective pitch and at each airspeed. A similar program was conducted for the helicopter without wings but with auxiliary propulsion. Resulting was a fairly complete matrix of 68 data points, which was used to evaluate the parametric effects of rotor lift, drag, and advance ratio on the entire dynamic system.

Data reduction consisted of converting the analog flight tape to digital form and tabulating time history and harmonic data for the 90 parameters of each flight condition using digital computer programs. In addition, certain calculations were required to transpose the aerodynamic pressure data to airloading by integration over the chord, to define total vibratory blade stresses and moments, and to form rotor hub forces from the blade root response data. In order to attain sufficient accuracy of the harmonic data, 72 data points per revolution (every 5° of azimuth) were used. The resulting large quantity of data made the automatic data processing necessary.

Analytical Methods

The data reduction process included calculation of blade airloads and main rotor hub forces using the digital computer programs. The analytical methods applied are described herein.

Main Rotor Blade Airloads

Airloads were calculated from the measured pressures using a Gaussian integration over the blade chord. The integration was based on obtaining differential pressure across the blade at 4.2, 15.8, 30.0, 60.0, and 91.0% chord (measured from the leading edge). Before performing the integration, differential pressure was formed at blade locations where two absolute pressure measurements were made. Airloads were calculated at 40, 75, 85, 95, and 98% blade spans.

Main Rotor Hub Forces

Hub forces were determined from measured blade root data. Calculation of hub forces in the nonrotating axis system, starting from measurements on the blade, is shown schematically in Fig. 2. Four steps are used in the calculation of these forces: 1) Calculation of blade forces near the root (forces near the blade root are determined by considering an instrumented segment as a free body and solving for the unknown forces). 2) Calculation of forces at the hinge in the hub system (inertia correction terms of the blade cuff are included and the resulting hinge forces transferred to the hub system). 3) Calculation of rotating hub forces due to all blades (all blade forces are added to form rotating hub forces). 4) Calculation of hub forces in the nonrotating system (the hub forces are transferred to the nonrotating system).

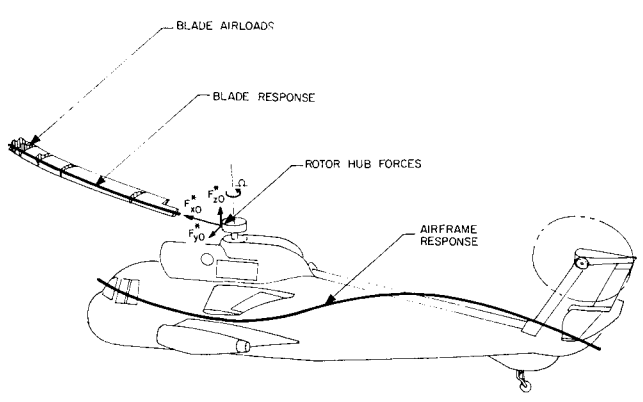

Fig. 1 Aircraft instrumentation.

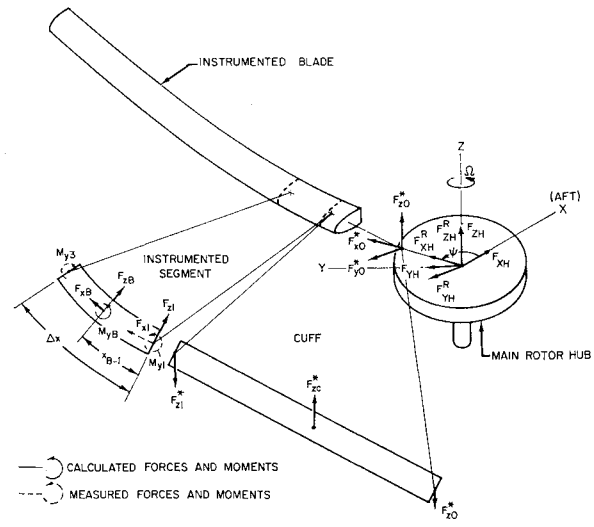

Fig. 2 Main rotor hub force calculation.

Calculation of blade forces near the root

Measured blade root data were used to analyze the forces and moments acting on a section of the blade. This method is referred to as the root response method. This analysis, developed by UACRL, was modified to improve the dynamic treatment of the blade root by including rotor head motion and other refinements. The basic approach is to define the forces and moments acting on an instrumented segment (I.S.) near the root of one main rotor blade. The location of the I.S. with respect to the main rotor hub is shown in Fig. 2. By taking the summations of moments about the outboard end of the I.S. (station 3) in the flatwise and edgewise directions, it is possible to solve for the vertical and edgewise blade system forces at the inboard end (station 1). Figure 2 shows the forces and moments that enter into the flatwise moment equation. Because of the relatively stiff cuff, the blade is assumed rigid out to the inboard end of the I.S. Because of the structural configuration of this segment, the edgewise bending is assumed negligible compared to the flatwise bending. Therefore, taking the summation of flatwise moments about station 3 and solving for the flatwise blade force at station 1 result in

$$F_{z1} = -\frac{1}{\Delta x}(M_{y1} + M_{yB} - M_{y3}) - \frac{F_{xB}(\Delta x - x_{B-1})}{\Delta x} + \frac{F_{x1}z_3}{\Delta x} + \frac{F_{xB}}{\Delta x}\left\{z_3 - \left[z_B + \left.\frac{\partial z}{\partial x}\right|_B (\Delta x - x_{B-1})\right]\right\} \quad (1)$$

Similarly, summing edgewise moments and solving for the edgewise station 1 force give

$$F_{y1} = (1/\Delta x)(M_{z1} + M_{zB} - M_{z3}) - F_{yB}(\Delta x - x_{B-1})/\Delta x \quad (2)$$

Equations (1) and (2) along with the measured blade tension at station 1 ($-F_{x1}$) determine the blade system orthogonal forces at the inboard end of the I.S. The UACRL-developed equations of motion, modified to include rotor head motion, provide the inertia force and moment terms (subscript B) in Eqs. (1) and (2). The rest of the variables are known from the I.S. geometry or are measured as dynamic

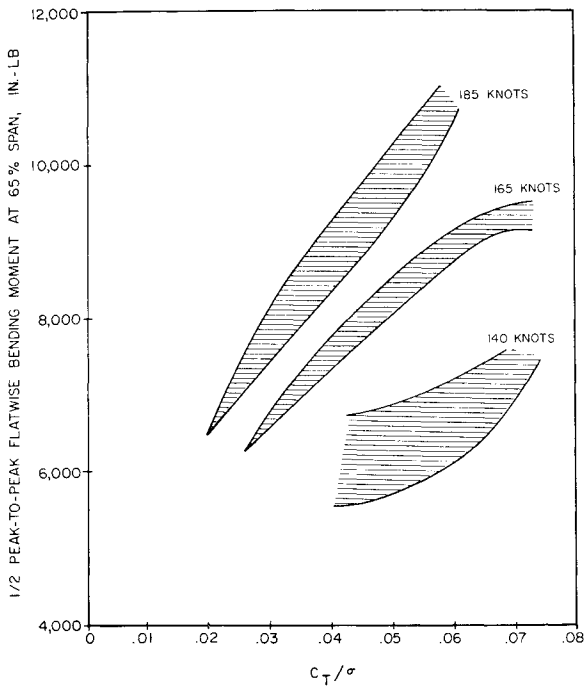

Fig. 3 $\frac{1}{2}$ peak-to-peak flatwise bending moment (in.-lb) at 65% span vs C_T/σ.

data. The required measurements are the flatwise and edgewise bending moments at each end of the I.S., the blade tension at station 1, the blade root angles with respect to the hub (lag, flap, and pitch), and the rotor head acceleration response. Equations (1) and (2) are expanded by using the inertia force and moment equations. They contain all the dynamic force terms and become quite involved.

Calculation of forces at the hinge in the hub system

The hinge forces are obtained by taking into account the inertia forces of the blade cuff mass. The cuff is the part of the blade between station 1 and the blade lag-flap hinge. These forces F_{xc}, F_{yc}, and F_{zc} are calculated again using the modified equations of motion. The station 1 forces given by Eqs. (1) and (2) and the measured tension along with the cuff inertia forces are then transformed from the blade axis system to the hub axis system using the measured blade root angles. As can be seen from Fig. 2 for the flatwise direction, the root shear forces due to one blade are found by summing the forces acting on the cuff segment. This determines the rotating hub system radial, tangential, and vertical hinge forces (F_{x0}*, F_{y0}*, and F_{z0}*) due to one blade acting on the rotor hub.

Calculation of rotating hub forces due to all blades

The hub forces in the rotating system are calculated by adding the force effects due to all of the b main rotor blades (b = 5 for the NH-3A). Assuming each blade has the same azimuthal history of hinge forces as does the instrumented blade, it can be shown that the rotor acts as a filter, the rotor shaft experiences only certain harmonics of the hinge forces, and all other harmonics cancel. Vertically, only kbth (steady, fifth, tenth, etc. for the NH-3A)harmonic forces are felt by the shaft in the rotating system. In the in-plane rotating directions of the hub, only $kb \pm 1$th (first, fourth, sixth, etc. for the NH-3A) harmonic forces can exist at the shaft due to the effects of all blades. All other harmonics cancel when the effects of all blades are considered. Figure 2 shows these rotating hub forces, $F_{XH}{}^R$, $F_{YH}{}^R$, and $F_{ZH}{}^R$. The same filtering results for moments about the three axes.

Calculation of hub forces in the nonrotating system

Nonrotating hub forces F_{XH}, F_{YH}, and F_{ZH} are determined by transforming the rotating system hub forces to the nonrotating axis system at the main rotor shaft. This is a transformation in the in-plane directions due to the 1/rev main rotor frequency. The nonrotating vertical hub forces are exactly the same as the rotating forces, i.e., steady, fifth, tenth, etc. harmonics for the NH-3A. In the in-plane directions, fourth and sixth harmonic components in the rotating system result in fifth harmonic components in the nonrotating system, ninth and eleventh harmonics result in tenth harmonic, and so on. Therefore, in each of the three orthogonal nonrotating axes at the shaft, only steady, fifth, tenth, etc. harmonics of forces exist for the NH-3A. For this program, only the steady and fifth harmonics were calculated since the higher harmonics are of much smaller magnitude. The forces are shown in Fig. 2.

The total nonrotating shaft forces were found by adding the inertia effects of rotor head motion to the hub forces. The nonrotating system inertia forces exist only at the kb/rev frequencies for the steady-state level flight conditions that were considered in this program.

The method of determining hub forces described previously provided additional insight into the transfer of forces from blade to hub over previous methods of direct shaft or hub measurement.

Discussion of Results

Study of the effects of rotor loading on the dynamic response mechanism has revealed some interesting trends. Increasing rotor lift or advance ratio increased blade stress and rotor loads significantly. Sensitivity to rotor propulsion/drag was found to be less pronounced.

Sensitivity of Flatwise Bending Response

Maximum stress in articulated rotor blades occurs near the midspan. The primary contributor to blade stress is flatwise bending. Flatwise bending moment at 65% span was therefore studied. Vibratory bending moment is plotted vs rotor lift (C_T/σ) in Fig. 3 for three speed regimes (140, 165, and 185 knots). The scatter shown by the width of the bands reflects the effect of rotor propulsion. Increasing rotor lift or advance ratio significantly increased blade bending whereas variation in rotor propulsion had a lesser effect.

The effects of rotor lift and rotor propulsion on blade bending at 140 knots are shown in Fig. 4. Contours of constant amplitude bending moment are shown as functions of rotor lift and propulsion. Such contours are useful for picturing trend effects. Evident is the greater sensitivity to C_T/σ than to C_D/σ. The amplitude of the first harmonic is greater than that of the higher harmonics. However, the second and third harmonics define the signature of the total $\frac{1}{2}$ peak-to-peak bending moment contours. Contours of the first three harmonics are plotted as functions of C_T/σ and C_D/σ for the 140 knot flight regime in Fig. 5. Note that the first harmonic amplitude is insensitive to variations in lift or propulsion.

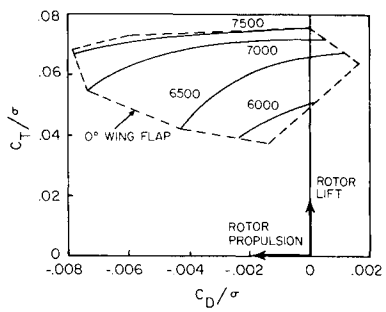

Fig. 4 Contours of constant $\frac{1}{2}$ peak-to-peak flatwise bending moment (in.-lb) at 65% span at 140 knots.

The contour lines for the second and third harmonics are closer together. Although the actual magnitudes of these harmonics are lower than that of the first, it is clearly their sensitivity to lift and drag that defines the similar shape for the $\frac{1}{2}$ peak-to-peak contours shown in Fig. 4.

Sensitivity of Rotor Hub Forces

The 5/rev vibratory hub forces in the nonrotating system result from 4, 5, and 6/rev loads in the rotating system. The 5/rev hub loads are sensitive to not only the amplitude of the rotating system forces but to their phase as well. A meaningful investigation of these parametric sensitivities of rotor loads requires study of the interrelated terms and is too extensive to be presented here. However, some significant gross effects can be clearly seen in Fig. 6. Shown are the amplitudes of the nonrotating system 5/rev forces in the lateral, longitudinal, and vertical directions as a function of airspeed. The width of the bands reflects the combined effects of rotor lift and propulsion. Note that the vertical force is independent of airspeed whereas in-plane forces are extremely sensitive to airspeed. The lateral force tripled in amplitude from 140 to 185 knots. The longitudinal force also increased with airspeed though less significantly. The key to reducing vibration at high speeds with this rotor system lies in the in-plane direction and therefore with 4 or 6/rev rotating system forces. This is substantiated in part by the success of the 4/rev tuned in-plane rotor head absorber currently on commercial versions of the S-61 helicopter.

Analytical Studies

Two analytical studies were performed. The ability of rotor dynamic analyses to correlate with measured airloads, blade response, and rotor hub forces was evaluated. The significant terms contributing to the 5/rev hub forces were determined.

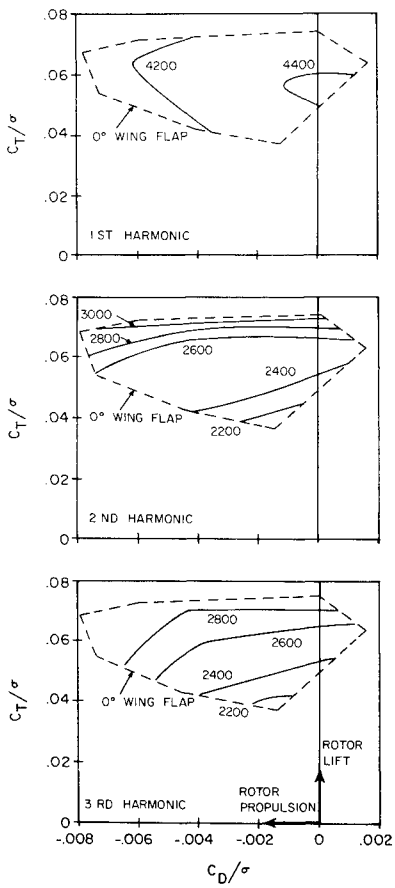

Fig. 5 Contours of harmonics of flatwise bending moment (in.-lb) at 65% span at 140 knots.

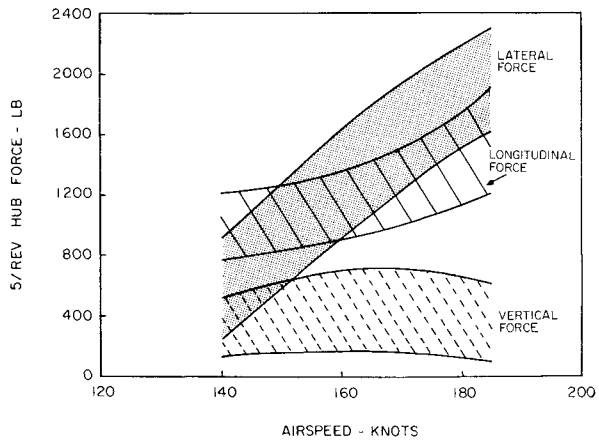

Fig. 6 Effect of airspeed on 5/rev hub forces.

Analytical Correlation Study

Analytical methods were used to predict the aerodynamic environment, and the response of the rotor system to this aerodynamic excitation. A nondistorted wake variable inflow analysis was used in conjunction with a lumped mass rotor dynamic response analysis. In earlier studies, the inflow was considered to be uniform through the rotor disk. This assumption, adequate for performance prediction, was found to lack the higher harmonic contribution required to define n/rev vibration. In order to improve the higher harmonic analytical capability, a variable inflow distribution was defined based on circulation of the elements of the rotor wake. This is the analysis evaluated here. It assumes that the wake is not distorted as it travels behind and below the advancing rotor, but retains its original spacing.

In order to evaluate a highly loaded rotor, a 142 knot flight condition, flown without auxiliary propulsion, was chosen for correlation. The rotor lift was 18,300 lb and the rotor propulsion was 1340 lb. In the following subsections, the correlation of the aerodynamic loading distribution, the blade bending response, and finally the resulting vibratory hub loads are studied.

Airload correlation

An analysis of airload correlation can be made by evaluating the time histories of airload and by studying the resulting harmonics. Test and analytical airloads are plotted vs azimuth angle $\psi = \Omega t$ in Fig. 7 at each span station where airloads were measured. The least correlation appears in the advancing blade quadrant. In general, the correlation is better inboard than at the tip of the blade. The greatest discrepancy is at the blade tip (98% span). There the major cause of the differences is the steady value of airload. This can be seen more readily from the harmonic definition of airload shown in Fig. 8. The steady value of the blade tip airload is off by 2 to 1 whereas the harmonics of interest are much better. The blade tip steady airload discrepancy can be explained by steady pressure shifts in the transducers. Differential pressure transducers were used to define the entire chordwise pressure distribution at the 98% span station only. Absolute pressure gages were used for the inboard stations. The differential gages are more sensitive to steady shifts in temperature that affect the steady offset. Dynamic pressures of both gages are relatively insensitive to temperature variation. Though the analytical and test airloads were compared directly, they can best be evaluated by studying the resulting blade and hub responses.

Blade response correlation

The correlation of vibratory stress is shown in Fig. 9. Flatwise and edgewise stresses are plotted vs span. Correlation

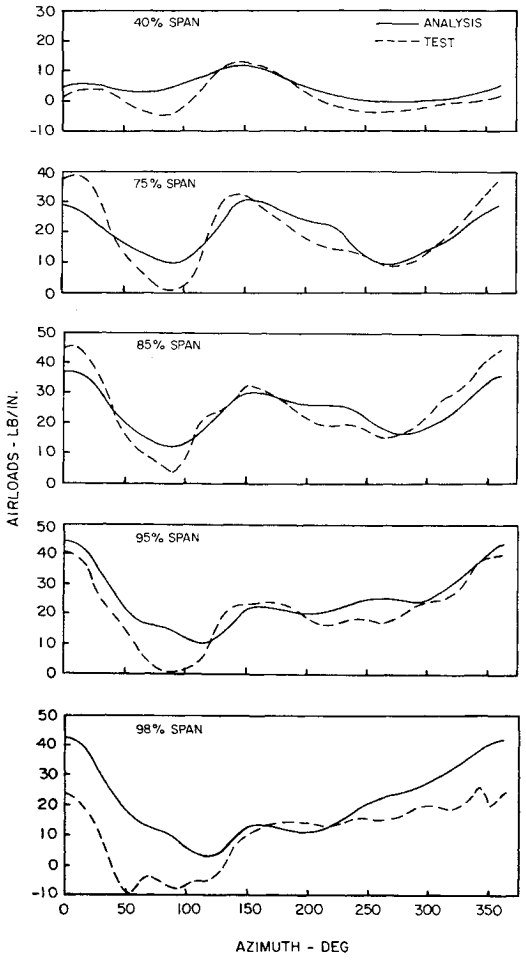

Fig. 7 Airload distribution at 142 knots.

of harmonics of stress is not shown here due to space limitations, but the improvement in edgewise correlation over previous studies was of prime interest. A major improvement in the analysis was the inclusion, for each harmonic, of separate values of lag damper characteristics that were obtained from the flight data.

Vibratory blade root shear correlation

Harmonics of the vertical and tangential shear at the root of the blade are shown in Fig. 10. The steady and first harmonics define the trim of the aircraft (rotor lift, drag, torque, and head moment). The fifth vertical and the fourth and sixth tangential harmonics are of primary interest since only they are transferred as forces to the airframe. Most harmonics are predicted within 30% of the test data. Previous studies, with the constant inflow assumption, have predicted rotor loads which were orders of magnitude lower.

Evaluation of the Root Response Method

The objective of this study was to evaluate the hinge force measurement technique and to determine the principal elements forming the rotating system hinge forces. The fifth out-of-plane (vertical) and the fourth and sixth in-plane (radial and tangential) harmonics of the rotating hinge forces were investigated since these are the forcing frequencies resulting in fixed system fifth harmonic forces for the 5-bladed NH-3A rotor system. The root response method discussed previously was used to obtain these forces. The results of applying this method are discussed in this section.

Vertical hinge force

Evaluation of the terms comprising the total vertical hinge force revealed that the one term $F_{z1}\sin\beta$ is a good approximation of the total fifth harmonic vertical force. This term was found to consist primarily of $T_0\beta_5$, i.e., steady tension $\times$ the fifth harmonic of blade flapping. Although there are other terms that are significant by themselves, an unexplained cancellation was found to minimize their combined effect for the fifth harmonic. It was also found that $T_0\beta_n$ is the predominant term for the first three harmonics.

In-plane radial hinge force

The radial hinge force is obtained from the measured blade tension at the instrumented segment. However, the placement of the tension measurement necessitates the addition of cuff correction terms to account for radial forces generated inboard of the tension measurement. The two dominant terms comprising the total force are the measured tension transferred to the hub axis system and cuff inertia due to rotor head motion. The measured tension term actually forms the total radial hinge force for all harmonics except the fourth and sixth. Since, for steady-state conditions, the hub can oscillate in the in-plane directions only at $(kb\pm1)$/rev, the hub accelerations and resulting cuff inertial forces were zero for all but the first, fourth, and sixth harmonics. It was found that for the sixth harmonic the measured vibratory tension term and the cuff inertia term were in phase, indicating that the measured sixth harmonic tension force is due primarily to rotor hub motion. This is not true for the fourth harmonic where a phase difference between these terms indicates the source of the fourth harmonic measured tension force is other than pure inertia force due to hub motion. This was expected because the proximity to 4/rev resonance of the first edgewise bending mode results in much greater edgewise response to 4/rev than to 6/rev. Increased edgewise response gives rise to radial forces through vibratory variation in centrifugal force that add to the inertial forces due to hub motion.

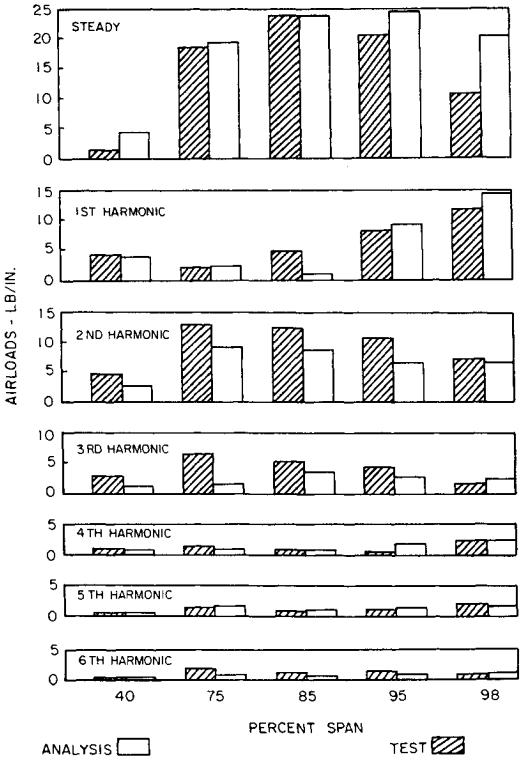

Fig. 8 Harmonics of airloads (test and analysis) at 142 knots.

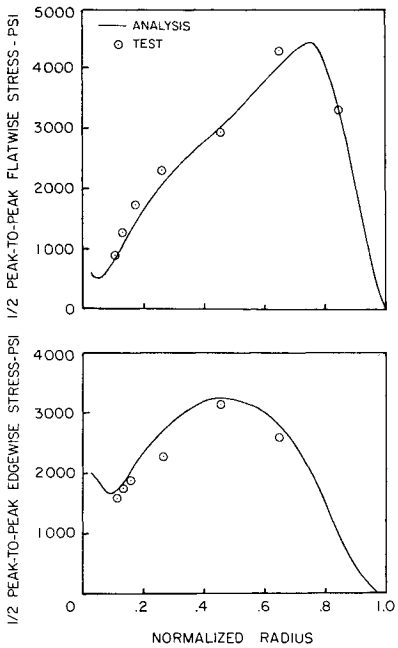

Fig. 9 Spanwise distribution of ½ peak-to-peak flatwise and edgewise stresses at 142 knots.

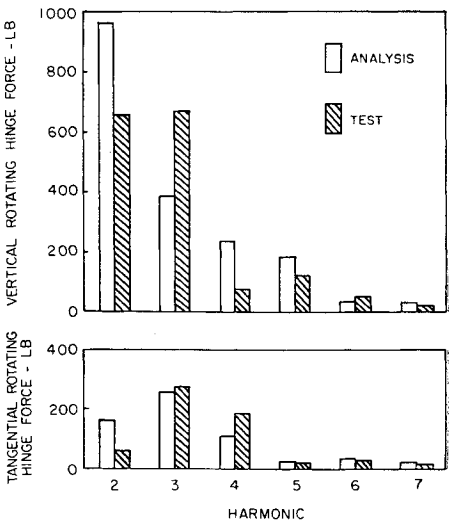

Fig. 10 Harmonics of analysis and test vertical and tangential rotating hinge forces at 142 knots.

In-plane tangential hinge force

In general, a greater number of significant terms were required for definition of the force in the tangential direction than in the vertical and radial directions. The term $F_{x1} \sin\gamma$ is the predominant force for only the first two harmonics. Defining the primary fourth and sixth harmonics of the tangential force requires the addition of $F_{x1} \sin\gamma$, cuff inertia due to hub motion, differential blade bending moment, and lag angular acceleration terms.

Conclusions

Semiconductor Pressure Transducers

The miniature transducers developed by Scientific Advances Inc. satisfactorily measured vibratory aerodynamic pressure under the severe environmental effects of a rotating rotor blade. However, the steady aerodynamic pressures of several transducers, primarily some of the differential transducers, exhibited zero shift due to temperature and other environmental effects.

Parametric Effects on 5/rev Rotor Hub Forces

The in-plane (longitudinal and lateral) forces are much higher than the vertical forces, especially at high airspeed. Increasing airspeed significantly increases the in-plane forces but does not affect the vertical hub force. Increasing rotor lift increases all hub forces.

Parametric Effects on Vibratory Blade Response

Increasing airspeed increases total vibratory flatwise blade stresses. Increasing rotor lift increases, the total vibratory flatwise bending moment and all harmonics except the first. Total vibratory flatwise moment is generally independent of rotor drag.

Analytical Correlation

Correlation of airloads, blade response, and root shear forces was demonstrated between the measured and analytical data. Improvements over earlier correlation studies were evidenced.

Evaluation of the Root Response Method

The blade root response method of measuring hub forces was successful. Evaluation of the major terms contributing to the fourth, fifth, and sixth harmonics of hinge forces, which form the fifth harmonic nonrotating hub forces for the 5-bladed NH-3A, revealed the following:

1) *Vertical hinge force*: The total vertical fifth harmonic force is approximated very well by one term—steady tension $\times$ 5/rev blade flapping.

2) *In-plane radial force*: The fourth and sixth harmonics of radial force are comprised basically of two terms—measured tension transferred to the hub axis system and cuff inertia force due to rotor head motion.

3) *In-plane tangential force*: Adequate definition of the fourth and sixth harmonics of tangential force requires the addition of $F_{x1} \sin\gamma$, cuff inertia due to hub motion, differential blade bending moment, and lag angular acceleration terms.

References

[1] Pruyn, R. R., "In-Flight Measurement of Rotor Blade Airloads, Bending Moments, and Motions, Together with Rotor Shaft Loads and Fuselage Vibration, on a Tandem Rotor Helicopter-Volume IV Summary and Evaluation of Results," USAAVLABS 67-9D, Nov. 1967, U.S. Army Aviation Materiel Labs., Fort Eustis, Va.

[2] Bartsch, E. A., "In-Flight Measurement and Correlation with Theory of Blade Airloads and Responses on the XH-51A Compound Helicopter Rotor—Volume I Measurement and Data Reduction of Airloads and Structural Loads," USAAVLABS 68-22A, May 1968, U.S. Army Aviation Materiel Labs., Fort Eustis, Va.

[3] Fenaughty, R. R. and Beno, E. A., "NH-3A Vibratory Airloads and Vibratory Rotor Loads," Naval Air Systems Command Rept., to be published.